

Residual Strength of Panels with Cracks Based on a Plastic Hinge

Eric J. Hein*

Cessna Aircraft Company, Wichita, Kansas 67215-1424

and

Bert L. Smith†

Wichita State University, Wichita, Kansas 67260-0044

DOI: 10.2514/1.26834

The residual strength of a panel with a crack is dependent on the mode of failure. Generally, the panel will exhibit a brittle-fracture mode of failure (based on linear elastic fracture mechanics) or a mode of failure based on yielding. A common practice is to assume an elastic, perfectly plastic, material behavior, along with a net-section-yield criterion for panels that fail by yielding. However, the net-section-yield criterion is not appropriate for configurations such as panels with asymmetric geometry or loading, because equilibrium is violated. For asymmetric cases such as panels with edge cracks or off-center cracks, a plastic moment or hinge must exist, the details of which may be determined by satisfying equilibrium. The purpose of this study is to compare the experimental residual strengths of panels with edge cracks and off-center cracks with the residual strengths determined from the assumption of elastic, perfectly plastic, behavior and a plastic-moment (hinge) criterion. The material chosen for this study is 2024-T3 aluminum alloy. This material is commonly used for aircraft skin and it has a high fracture toughness, and so the mode of failure will less likely be brittle fracture. An elastic, perfectly plastic, material model was assumed, and expressions were developed for a plastic-hinge failure for panels with edge cracks as well as off-center cracks. A large number of panels with either edge cracks or off-center cracks were tested to failure, and the results were compared with the results obtained from the equations developed from the plastic-hinge assumption. The results from the plastic-hinge assumption compared favorably with the experimental results.

Nomenclature

a	= crack length for edge crack; half-crack length for off-center crack
a_f	= final crack length
b	= specimen half-width
c	= symmetrical crack moment arm
d	= crack offset
e	= crack edge distance
F_{ty}	= allowable tensile yield stress (0.2% offset)
F_{tu}	= allowable tensile ultimate stress (corresponding to engineering strain)
ℓ	= total crack length ($2a$ for a center crack)
P_{crit}	= critical load
σ	= applied (remote) stress
σ_c	= critical stress
σ_{ys}	= yield stress
t	= thickness
w	= specimen width

Introduction

THE residual strength of an aircraft structure such as an aluminum skin panel with a crack is determined by calculating the lowest critical stress based on brittle fracture or yield. Brittle fracture is driven by the fracture toughness of the material, and yield is driven by the yield strength of the material. Both failure mechanisms are also highly dependent on geometry. For highly

ductile materials such as 2000 Series aluminum, yielding is often dominant for other than very wide specimens. Most rough-analysis methods and commercially available software packages use simplistic analysis to calculate the critical stress due to yielding. Often an elastic, perfectly plastic, material is assumed and a net-section-yield criterion is applied. The equation used to calculate the critical stress due to net section yield is given as follows:

$$\text{net section strength} = \frac{\text{area (net)}}{\text{area (gross)}} (\text{yield strength}) \quad (1)$$

The widely used Air Force Growth (AFGROW) software calculates the critical net-section-yield stress as follows [1]:

$$\begin{aligned} \text{net section strength} \\ = \frac{(\text{width} - \text{diameter} - \text{crack length} - \text{plastic zone})}{\text{width}} (\text{yield strength}) \end{aligned} \quad (2)$$

The AFGROW method simply takes the basic calculation [Eq. (1)] one step further by adding the plastic-zone size to the crack length. This simplistic approach requires two assumptions to be made: 1) the material behaves as an elastic, perfectly plastic, material and 2) the geometry and loading are symmetric. Consequently, only center-cracked or symmetrically double edge-cracked specimens would meet this criteria.

In contrast to Eqs. (1) and (2), numerous, more complex, methods have been developed to more accurately predict ultimate failure. Algorithms for predicting the fracture-failure history of center-cracked panels are outlined in [2,3]. Ghassemieh et al. [2] uses a plasticity analysis (the von Mises yield criterion) combined with removing nodal connectivities for elements with effective stresses above the ultimate failure stress. As the author refines the mesh, it slowly converges toward the experimental ultimate failure stress. The development of a fracture-analysis technique for use with general-purpose finite element analysis software is given in [4]. Cordes [4] uses nonlinear springs to model the cohesive forces

Received 28 July 2006; revision received 24 January 2007; accepted for publication 14 February 2007. Copyright © 2007 by the American Institute of Aeronautics and Astronautics, Inc. All rights reserved. Copies of this paper may be made for personal or internal use, on condition that the copier pay the \$10.00 per-copy fee to the Copyright Clearance Center, Inc., 222 Rosewood Drive, Danvers, MA 01923; include the code 0021-8669/07 \$10.00 in correspondence with the CCC.

*Senior Engineer, Structures, One Cessna Boulevard. Member AIAA.

†Professor, Department of Aerospace Engineering, 1845 Fairmont. Senior Member AIAA.

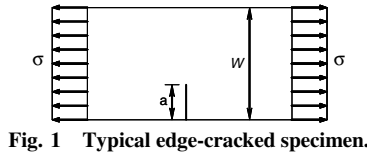


Fig. 1 Typical edge-cracked specimen.

between the sides of the given crack path within an assumed process zone. Alternately, local values of the strain energy density are used in [5] to characterize stable crack growth. Gdoutos [5] calculates the final stable crack length and ultimate failure load for a center-cracked panel by determining the critical amount of strain-energy-density absorption. These methods, although effective, are computationally intensive and time-consuming. This limits their practicality and likelihood of implementation in industry. Moreover, with the exception of [6], nearly all of the literature reviewed on predicting failure due to crack growth (tearing) in ductile materials addresses the center-cracked-panel configuration.

For an edge-crack configuration (Fig. 1), it is not possible to account for the moment created by the eccentricity of the panel using Eqs. (1) and (2). Also, it is not prudent to employ a rigorous finite element solution for each situation. Therefore, the simplistic prediction methods should be altered to account for eccentricity. One option is to assume that the specimen becomes a perfectly plastic hinge at failure. This option, called the *plastic-hinge method*, is shown experimentally through static testing herein to be a good predictor of the ultimate failure load for a panel. This paper will provide a description of the plastic-hinge method, present a comparison of this method with the experimental results from edge-cracked and off-center-cracked specimens, and offer suggestions for altering the plastic-hinge method to more accurately predict the critical loads.

Plastic-Hinge Method

A standard residual (critical) strength plot typically contains two curves: a net-section-yield curve and a brittle-fracture curve. The lower of the two curves is considered critical. Other corrections (such as the Feddersen [7] tangent line, which is a correction to the brittle-fracture curve for small crack lengths) can be made to this plot when appropriate. The net-section-yield critical portion of this curve can be unconservative for panels with edge cracks and off-center cracks. For an edge crack in a panel with a pinned support, a curve based on the plastic-hinge approach was overlaid on a residual strength plot in Fig. 2 to illustrate this point. Notice that in this case, brittle fracture is never critical when compared with the plastic-hinge curve; however, a portion of it is critical when compared with the net-section-yield curve.

Figure 3 gives the general specimen configurations used in this study for an edge crack (left) and an off-center crack (right). Note that an off-center crack has an additional parameter d .

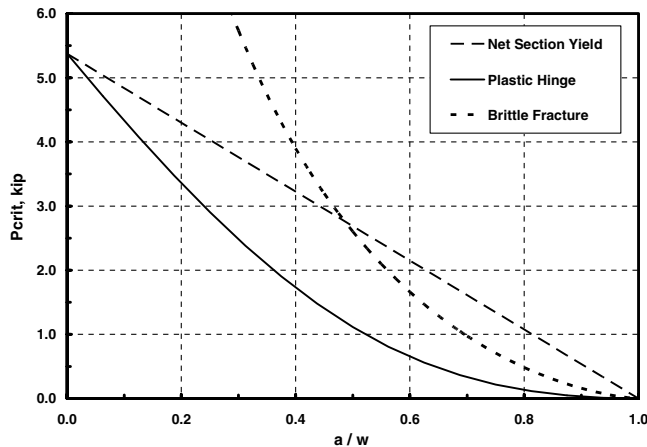


Fig. 2 Residual strength plot, edge-cracked specimen; pinned support.

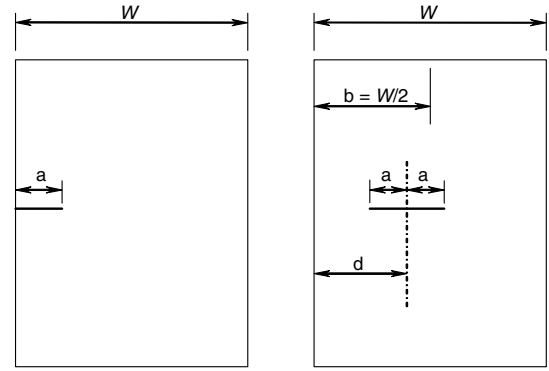


Fig. 3 Edge- and off-center-cracked specimen test-section nomenclature.

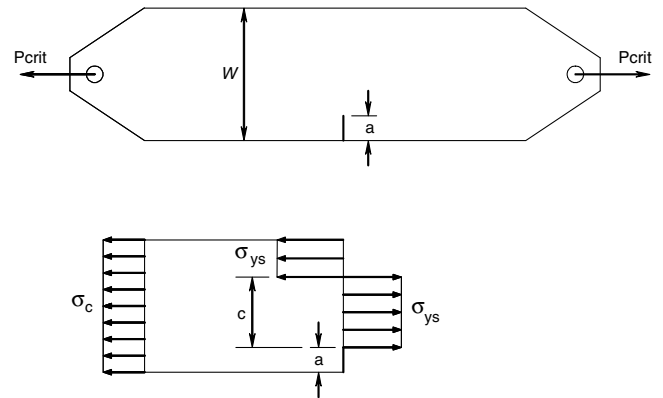


Fig. 4 Edge-cracked specimen and free-body diagram.

Based on the assumption of an elastic, perfectly plastic, material, the critical load based on a plastic hinge can be determined for an edge crack by simply requiring equilibrium for the free-body diagram given in Fig. 4. The summations of forces and moments are required to be zero, as shown in Eqs. (3) and (4):

$$\sum F = 0 = \sigma_c(w)t + \sigma_{ys}(w - a - c)t - \sigma_{ys}(c)t \quad (3)$$

$$\sum M = 0 = \frac{w}{2}(\sigma_c)(w)t + \left\{ a + c + \frac{1}{2}(w - a - c) \right\} \times (\sigma_{ys})(w - a - c)t - \left(a + \frac{c}{2} \right)(\sigma_{ys})(c)t \quad (4)$$

When Eqs. (3) and (4) are solved simultaneously for σ_c and c , the resulting expression for the critical stress σ_c is as follows:

$$\sigma_c = \frac{(-a + \sqrt{2a^2 - 2aw + w^2})\sigma_{ys}}{w} \quad (5)$$

The critical value of the tensile force is

$$P_{crit} = \sigma_c(w)t \quad (6)$$

In a similar manner, the critical load based on a plastic hinge for an off-center crack can be determined by simply requiring equilibrium for the free-body diagram given in Fig. 5. The summations of forces and moments are required to be zero, as shown in Eqs. (7) and (8).

$$\sum F = 0 = \sigma_c(w)t + \sigma_{ys}(w - \ell - c - e)t - \sigma_{ys}(c)t - \sigma_{ys}(e)t \quad (7)$$

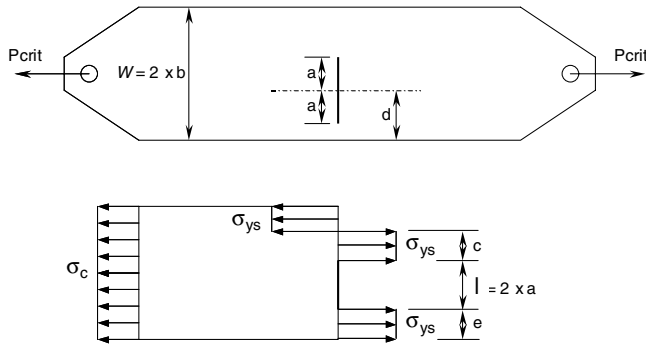


Fig. 5 Off-center-cracked specimen and free-body diagram.

$$\sum M = 0 = \frac{w}{2}(\sigma_c)(w)t + \left\{ \ell + e + c + \frac{1}{2} \times (w - \ell - e - c) \right\}(\sigma_{ys})(w - \ell - e - c)t - \left(\ell + e + \frac{c}{2} \right)(\sigma_{ys})(c)t - \frac{e}{2}(\sigma_{ys})(e)t \quad (8)$$

When Eqs. (7) and (8) are solved simultaneously for σ_c and c , the resulting expression for the critical stress σ_c is as follows:

$$\sigma_c = \frac{(-\ell + \sqrt{2\ell^2 + w^2 + 4\ell e - 2\ell w})\sigma_{ys}}{w} \quad (9)$$

where $e = d - \ell/2$ and $\ell = 2a$.

The critical value of the tensile force is the same as that given in Eq. (6).

This methodology can be applied to nearly any asymmetrical configuration, as long as the end restraints are known.

Static Testing

Static testing was conducted to validate the plastic-hinge analytical method. The test plan and test setup are described in this section. The goal of the static testing was to acquire predictable and repeatable results for as many configurations as possible. Based on the consistency of preliminary static testing of practice specimens, it was determined that just two replications are needed for each crack configuration. As a result, nine edge-crack and nine off-center-crack configurations were tested requiring a total of 36 specimens. Table 1 gives the test matrix for both the edge-cracked and off-center-

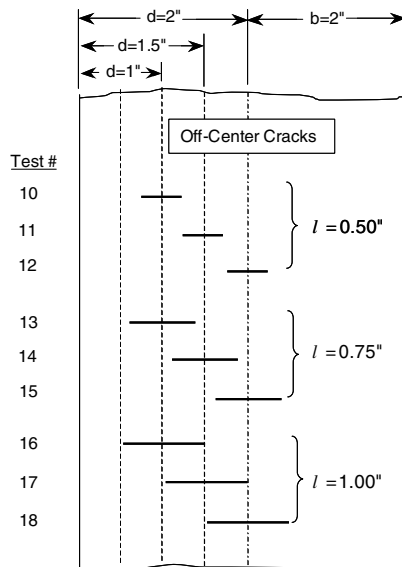


Fig. 6 Crack geometry for off-center cracks.

Table 1 Test matrix

Edge crack			Off-center crack			
Test	a , in.	Quantity	Test	ℓ , in.	d , in.	Quantity
1	0.10	2	10	0.50	1.00	2
2	0.20	2	11	0.50	1.50	2
3	0.30	2	12	0.50	2.00	2
4	0.50	2	13	0.75	1.00	2
5	1.00	2	14	0.75	1.50	2
6	1.50	2	15	0.75	2.00	2
7	2.00	2	16	1.00	1.00	2
8	2.50	2	17	1.00	1.50	2
9	2.75	2	18	1.00	2.00	2

cracked specimens. Both types of specimens were 4-in. wide, 0.032-in. thick, 14-in. long, and made from 2024-T3 bare sheet AMS-QQ-A-250/4 material. Figure 6 shows the crack geometry for the off-center test specimens 10 through 18, listed in Table 1.

The majority of the static testing was performed on a 5-kip-capacity MTS® static test machine. For several tests requiring loads above 5-kip, a 55-kip MTS machine was used. Each specimen was pulled to failure with a preset cross-arm rate of 0.02 in./min. The test-specimen geometry (without the crack) is shown in Fig. 7, and double-shear test fixtures employed for all tests are shown in Fig. 8. The specimens were sheared to the outer dimensions, and then the test sections and attachment holes were machined. All of the test specimens were machined from the same material lot. Furthermore, the grain direction runs perpendicular to the load direction for all test specimens, because most grain directions run parallel to the longitudinal axis of an aircraft and perpendicular to the hoop stress. Also, the mechanical properties for aluminum are typically lower in the long transverse direction than in the longitudinal direction for sheet material.

A saw cut was made in each specimen with a jeweler's saw, to create a crack of the desired length. For specimens with center cracks and off-center cracks, a hole was drilled at the center of the crack with a 1/16-in. drill bit, after which the saw blade was threaded through the hole, and saw cuts were made on each side of the hole to form the crack. For residual strength testing resulting in brittle fracture based on fracture toughness, the man-made cracks are usually fatigue-loaded before testing to sharpen the crack tips. However, for residual-strength testing resulting in failure from yielding, this is usually not required, because failure is assumed to be based on yield strength rather than fracture toughness.

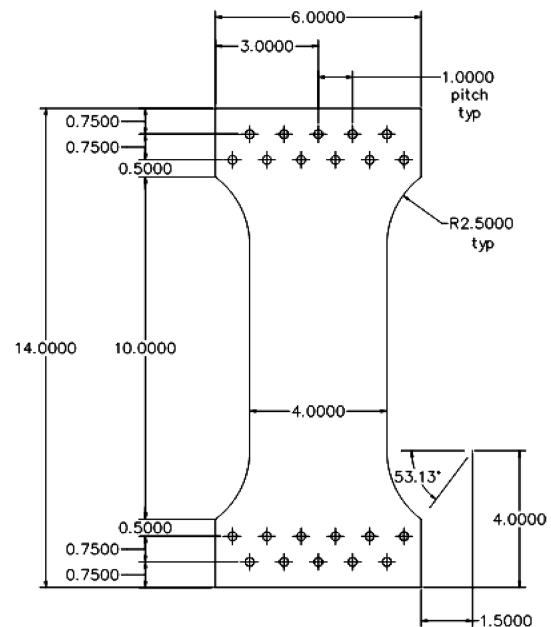


Fig. 7 Typical test specimen.

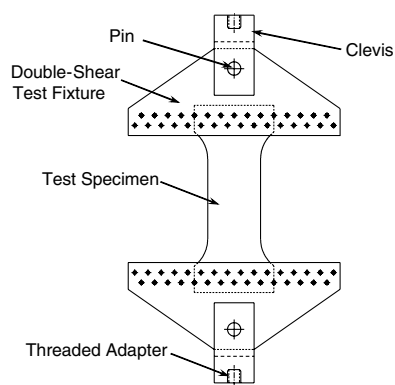


Fig. 8 Test fixture configuration.

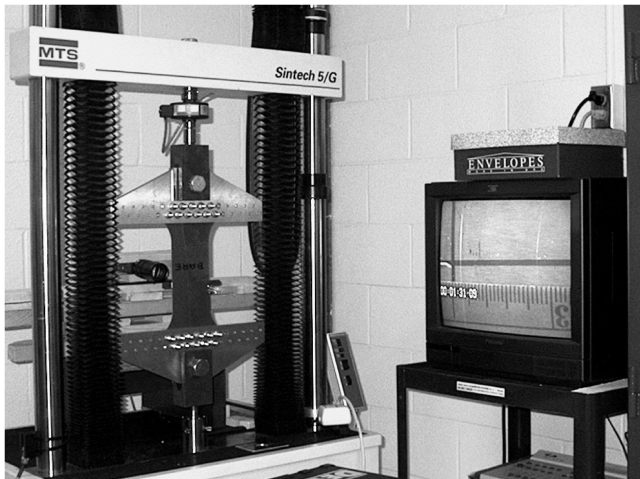


Fig. 9 MTS static test machine setup (5-kip capacity).

After the specimens were prepared, they were placed in the double-shear test fixtures and fastened down with 1/4-in. lag bolts. Next, the test specimen and fixture were placed into the upper clevis, and the load cell and cross-arm position readings were zeroed. Finally, the lower pin was placed in position, completing the test setup. Figure 8 shows the overall test-fixture configuration, including the test specimen, double-shear fixture, pin, and clevis.

The test setup for tests conducted on the 5-kip MTS machine also included a video camera with a 10X magnification lens, shown in Fig. 9. The camera was used to monitor the stable crack growth during testing; however, this information was not used in the analysis.

Test Results

Table 2 has the critical load determined experimentally for each of the edge-cracked test specimens and the average value of the critical

Table 2 Edge-crack test results

Test	a , in.	a/w	Test P_{crit} , lb		
			Specimen 1	Specimen 2	Average
1	0.10	0.025	6062	5949	6006
2	0.20	0.050	5409	5493	5451
3	0.30	0.075	4980	4988	4984
4	0.50	0.125	4204	4263	4234
5	1.00	0.250	2856	2882	2869
6	1.50	0.375	1810	1811	1811
7	2.00	0.500	893	899	896
8	2.50	0.625	381	385	383
9	2.75	0.688	241	248	245

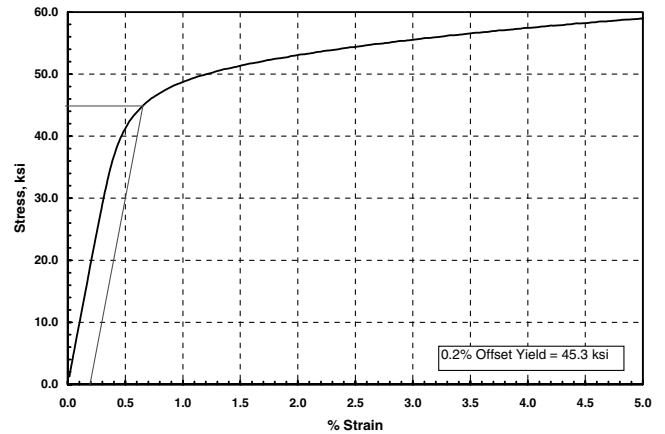


Fig. 10 Experimental stress-strain curve.

load. Table 3 has the critical load determined experimentally for each of the off-center-cracked specimens, along with the average value.

Because all of the test specimens were machined from the same material lot, an experimental value for yield strength was developed to create a baseline for comparison. Four tensile specimens were fabricated from the same material lot that was used to fabricate the test specimens. The tensile specimens were 0.5-in. wide, 8-in. long, and 0.032-in. thick. The grain direction for the tensile specimens was perpendicular to the loading direction, the same as the actual test specimens. The average experimental 0.2% offset yield stress was 45.3 ksi. In addition, the experimental ultimate failure stress was consistently 64 ksi. The resulting stress-strain curve is shown in Fig. 10.

Comparison of Test Results with Analytical Model

For each of the two configurations, the experimental values of the critical load are compared with the analytical values. The equations for the analytical values of the critical stress given by Eqs. (5) and (9)

Table 3 Off-center-crack test results

Test	a , in.	a/b	d , in.	d/b	Test P_{crit} , lb		
					Specimen 1	Specimen 2	Average
10	0.250	0.125	1.00	0.50	5151	5161	5156
11	0.250	0.125	1.50	0.75	5329	5330	5330
12	0.250	0.125	2.00	1.00	5347	5380	5364
13	0.375	0.1875	1.00	0.50	4327	4355	4341
14	0.375	0.1875	1.50	0.75	4695	4774	4735
15	0.375	0.1875	2.00	1.00	4853	4875	4864
16	0.50	0.250	1.00	0.50	3575	3607	3591
17	0.50	0.250	1.50	0.75	4147	4213	4180
18	0.50	0.250	2.00	1.00	4404	4454	4429

Table 4 Edge-cracked plastic hinge, % error vs test

a , in	a/w	Test P_{crit} avg., lb	Plastic hinge P_{crit} , lb: % error vs test					
			A-basis	% error	B-basis	% error	Experimental	% error
0.10	0.025	6006	5109	14.9%	5231	12.9%	5510	8.3%
0.20	0.050	5451	4845	11.1%	4961	9.0%	5226	4.1%
0.30	0.075	4984	4586	8.0%	4695	5.8%	4946	0.8%
0.50	0.125	4234	4080	3.6%	4177	1.3%	4400	3.9%
1.00	0.250	2869	2906	1.3%	2975	3.7%	3134	9.3%
1.50	0.375	1811	1902	5.1%	1948	7.6%	2052	13.3%
2.00	0.500	896	1113	24.3%	1140	27.2%	1201	34.0%
2.50	0.625	383	558	45.8%	572	49.3%	602	57.3%
2.75	0.688	245	364	48.8%	373	52.4%	392	60.5%
Mean percent error				18.1%		18.8%		21.3%
Standard deviation				17.9%		19.6%		23.4%

Table 5 Off-center-cracked plastic hinge, % error vs test

a/b	d/b	Test P_{crit} avg., lb	Plastic hinge P_{crit} , lb: % error vs test					
			A-basis	% error	B-basis	% error	Experimental	% error
0.250	1.00	4429	4032	9.0%	4128	6.8%	4349	1.8%
0.250	0.75	4180	3685	11.8%	3773	9.7%	3974	4.9%
0.250	0.50	3591	3312	7.8%	3391	5.6%	3572	0.5%
0.1875	1.00	4864	4368	10.2%	4472	8.1%	4711	3.1%
0.1875	0.75	4735	4110	13.2%	4208	11.1%	4433	6.4%
0.1875	0.50	4341	3838	11.6%	3929	9.5%	4139	4.6%
0.125	1.00	5364	4704	12.3%	4816	10.2%	5074	5.4%
0.125	0.75	5330	4533	14.9%	4641	12.9%	4889	8.3%
0.125	0.50	5156	4357	15.5%	4461	13.5%	4699	8.9%
Mean percent error				11.8%		9.7%		4.9%
Standard deviation				2.6%		2.6%		2.8%

depend upon the yield stress of the material. Three different values of yield stress were selected. Two of these are the A-basis and B-basis values of 42 and 43 ksi, respectively [8]. The third is the experimental value determined herein of 45.3 ksi.

Table 4 has the experimental critical loads for the edge-cracked specimens and the critical loads determined analytically based on the plastic-hinge method. The analytical values are based on the three different values of yield stress: A-basis, B-basis, and the experimental value determined herein. The percent error is relative to the average critical load from testing. In addition, Fig. 11 is a graphical comparison of the experimental critical loads for the edge-cracked specimens with the critical loads from the plastic-hinge analytical method for the edge-cracked configuration. The percent error is calculated as follows:

$$\% \text{ error} = \left| \frac{\text{experimental} - \text{analytical}}{\text{experimental}} \right| 100\% \quad (10)$$

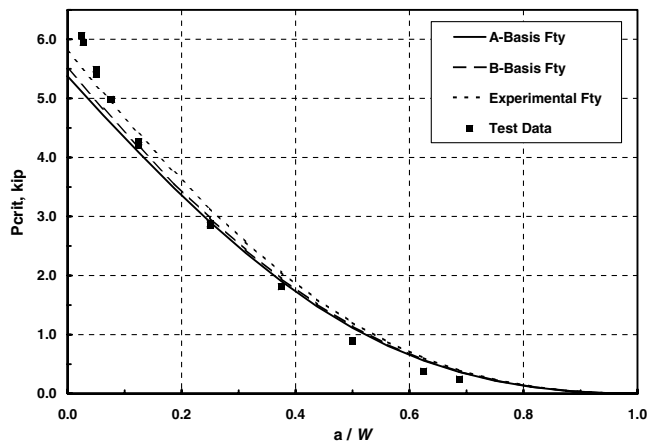
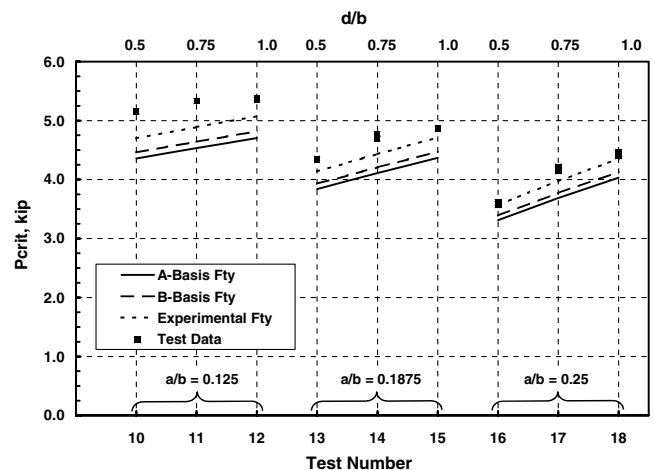
**Fig. 11 Edge-crack comparison.**

Table 5 has the experimental critical loads for the off-center cracks and the critical loads based on the plastic-hinge method for the off-center crack. Again, the analytical values are based on the three different values of yield stress. The percent error is again relative to the average critical load from testing. Figure 12 is a graphical comparison of the experimental critical load for an off-center crack, with the critical loads defined by the plastic-hinge method for A-basis, B-basis, and experimental values of the yield stress.

Empirical Correction to Analytical Model

Based on the comparison of the experimental values with the analytical values, the plastic-hinge method may be applied without an empirical correction for pin-loaded panels with edge cracks. The exception is for extremely short crack lengths for which the experimental values are higher than the analytical values, which is

**Fig. 12 Off-center-crack comparison.**

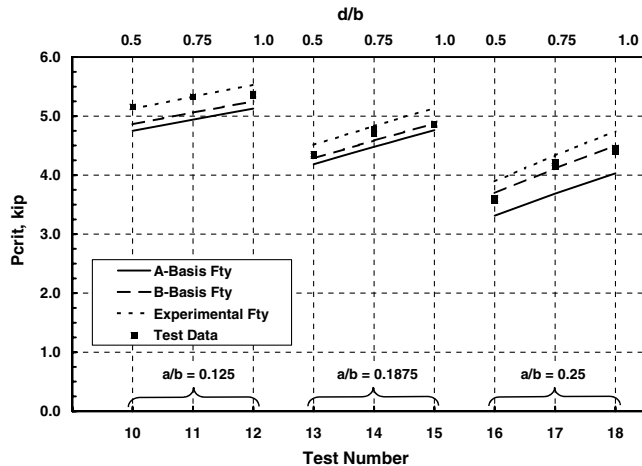


Fig. 13 Single scalar correction to an off-center crack.

logical because the critical value for a specimen with no crack should correspond to the ultimate strength of the material.

For pin-loaded panels with off-center cracks the mean percent error is 11.8% for an A-basis yield stress, 9.7% for a B-basis yield stress, and 4.9% for an experimental yield stress. Consequently, the mean percent error of all off-center-cracked panels that were tested is 8.8%. A single scaling factor equal to the overall mean percent error, which is approximately 9%, may be used to correct the plastic-hinge-model analytical results. That is, a multiplying (correction) factor of about 1.09 may be applied to the analytical results, which brings them in close proximity to the experimental results. The approach is simple and gives reasonable results, with an overall mean percent error of 3.1% and a standard deviation of 2.4%. Figure 13 gives a comparison of the corrected analytical model with test data for A-basis, B-basis, and experimental values of the yield stress for the off-center-crack configuration.

Conclusions

An elastic, perfectly plastic, approximation of stress vs strain and the concept of a plastic hinge were used to determine the residual strength of specimens with asymmetric crack geometry. The failure mode was yielding rather than brittle fracture. Edge-cracked and off-center-cracked specimens were used. Analytical models were developed for predicting the residual strength based on the elastic, perfectly plastic, assumption and the plastic-hinge concept, and the results were compared with residual strengths determined experimentally. The analytical models were developed in terms of the yield strength of the material. The analytical results for the edge-cracked specimens compared very favorably with the experimental results, except for very short cracks for which the strength of the panel approached the ultimate strength of the material rather than the yield strength. The analytical results for the off-center-cracked specimens were on the average about 9% lower than the experimental results. That is, if a multiplying factor of about 1.09 was applied to the analytical results, the average difference between analytical and experimental results was reduced to about 3.1%. It is important to point out that the average difference between analytical and experimental results for the off-center-cracked specimens was only 4.9% when using the yield strength value of 45.3 ksi determined herein rather than the A-basis or B-basis values.

Because the plastic-hinge method was successfully applied to multiple configurations, the method can be extended to additional, more complex, configurations. Portions of aircraft skin under tensile load that are narrow enough to be critical for yield, with some form of

eccentric crack, will have lower residual strengths than predicted by the net-section-yield method. Affected structures might include: the fuselage skin between windows or doors, manufacturing breaks, portions of skin in the cockpit region, lower wing or fuselage skin splices, flap island skins, etc. When evaluating more complex structures, an understanding of the stiffness of the surrounding structure is required. In the case of a flap island, the analyst would need to know the stiffness of the flap system and of the joint that attaches the flap island to the wing. Once the stiffness of the system is known, a free body of the system can be balanced and solved in a manner similar to the pin-loaded configuration. Pin-loaded configurations were chosen for this study because they are a worst-case scenario. As a result, a pin-loaded configuration can be conservatively assumed for most similar structures, providing no significant moment is applied.

To make the plastic-hinge model a more useful tool, additional work needs to be done. The full-range residual-strength curves for pin-loaded edge- and off-center-cracked test specimens must be better understood. A great deal of attention should be given to very small and very large crack lengths, because these are the regions with the highest percent of error. Furthermore, it would be beneficial to study a wide range of materials, panel widths, thicknesses, and boundary conditions. The plastic-hinge model is suitable for the configurations tested in this research; however, the model must be validated and/or altered for a wide range of configurations before implementation in industry.

The plastic-hinge model also has an effect on brittle-fracture analysis. Because thin panels are best represented by a plane-stress approximation, a plane-stress fracture-toughness value should be used in determining the critical stress due to brittle fracture. Center-cracked test specimens are typically used; however, an American Society for Testing and Materials standard for determining plane stress fracture toughness does not exist. Consequently, plane-stress fracture-toughness values developed using an eccentrically cracked panel must account for the bending moment on the test section of the specimen. To ensure brittle-fracture failure, the plastic-hinge model would require that much wider test specimens be used for eccentrically cracked panels than for center-cracked panels.

References

- [1] AFGROW, Software Package, Ver. 4.0009e.12, U.S. Air Force Research Laboratory, Analytical Structural Mechanics Branch (AFRL/VASM), Wright-Patterson AFB, OH, 2004.
- [2] Ghassemieh, M., Ali, M. S., and Kukreti, A. R., "Procedure to Predict Ultimate Fracture Failure History for Plane Stress Plasticity Problems," *Engineering Fracture Mechanics*, Vol. 41, 1992, pp. 919-933.
- [3] Miller, R. E., Backman, B. F., Hansteen, H. B., Lewis, C. M., Samuel, R. A., and Varnasi, S. R., "Recent Advances in Computerized Aerospace Structural Analysis and Design," *Computers and Structures*, Vol. 7, 1977, pp. 321-326.
- [4] Cordes, J., "Development of a Fracture Analysis Technique for Use with a General-Purpose Finite Element Program," Ph.D. Thesis, Stevens Inst. of Technology, Hoboken, NJ, 1989.
- [5] Gdoutos, E. E., "Stable Growth of a Central Crack," *Theoretical and Applied Fracture Mechanics*, Vol. 1, 1984, pp. 139-144.
- [6] Simonsen, B. C., and Tornqvist, R., "Experimental and Numerical Modeling of Ductile Crack Propagation in Large-Scale Shell Structures," *Marine Structures*, Vol. 17, 2004, pp. 1-27.
- [7] Feddersen, C. E., "Evaluation and Prediction of the Residual Strength of Centre Cracked Tension Panels," *Damage Tolerance in Aircraft Structures*, ASTM Special Technical Publication 486, American Society for Testing and Materials, Philadelphia, 1971, pp. 50-78.
- [8] Bakuckas, J., Jackson, J. L., Rice, R. C., and Thompson, S., "Metallic Materials Properties Development and Standardization (MMPDS)," Dept. of Transportation, Federal Aviation Administration Rept. AR-MMPDS-01, Jan. 2003.